

# MODELING THE HYDRODYNAMICS OF A TIDAL INLET DURING STORMS

L. Velasquez-Montoya<sup>1</sup>, A. Wargula<sup>1</sup>, J. Torres<sup>1</sup>, E. J. Sciaudone<sup>2</sup>, T. Tomiczek<sup>1</sup>, E. Smyre<sup>3</sup>

<sup>1</sup>Naval Architecture and Ocean Engineering Department, US Naval Academy, Annapolis, MD, USA. [velasque@usna.edu](mailto:velasque@usna.edu); [wargula@usna.edu](mailto:wargula@usna.edu); [m216744@usna.edu](mailto:m216744@usna.edu); [vjohnson@usna.edu](mailto:vjohnson@usna.edu)

<sup>2</sup>Department of Civil, Construction, and Environmental Engineering, North Carolina State University, Raleigh, NC, USA. [ejsciaud@ncsu.edu](mailto:ejsciaud@ncsu.edu)

<sup>3</sup>Dewberry, Raleigh, NC, USA. [esmyre@dewberry.com](mailto:esmyre@dewberry.com)

## 1. Introduction

Tidal inlets are strategic locations for the economic development and ecosystem well-being of barrier islands and coastal regions. Understanding of the processes that drive the hydrodynamics and morphology of tidal inlets is therefore needed to better manage sediment and infrastructure around these dynamic coastal features (Elko et al. 2020). Interaction of oceanic, estuarine, and atmospheric conditions make tidal inlets challenging to study, but it is known that the general circulation patterns of tidal inlets result from the balance of tidal, wind, and wave-induced currents (Bruun, 1978; Keulegan, 1967; de Swart and Zimmerman, 2009).

In recent decades, numerical models and observations have been combined to better understand the effects of waves in water level modulation in bays and areas surrounding tidal inlets. Dodet et al. (2013), Irish and Cañizares (2009), Olabarrieta et al. (2011), Orescanin et al. (2014), and Wargula et al. (2018) found that waves can reduce the ebb jet of inlets and increase water levels in the inlet mouth and bays. During ocean storms, the enhanced interaction of tidal flows and waves result in bathymetric changes along the inlet's main channel, ebb and flood deltas (Hopkins et al., 2018; Velasquez-Montoya et al., 2020) that in turn can modify circulation patterns after the storm.

Most of the studies that have looked at the response of tidal inlets during extreme conditions have focused on storms that propagate through the ocean; however, in large bays storms can travel landward of tidal inlets resulting in water levels in the bay exceeding those in the ocean. This work explores the effects of a synthetic storm that resembles the conditions of a major hurricane passing landward of a tidal inlet. The goal of this study is to gain insights on flooding extent, change in currents, and wave modulation of ebb discharge by bay-side storms. These insights can inform management practices of lands adjacent to tidal inlets as well as sediment management strategies within the inlet channel(s).

## 2. Study Area

Located in Dare County, North Carolina, and part of the barrier island system on the East Coast of the USA known as the Outer Banks, Oregon Inlet separates Bodie Island to the north and Hatteras Island to the south. It is the only inlet within nearly 210 km of shoreline between Rudee Inlet, VA to Hatteras Inlet, NC and provides access between the Albemarle-Pamlico Sound, the

Intracoastal Waterway, and the Atlantic Ocean. To facilitate navigation within the inlet, the U.S. Army Corps of Engineers (USACE) maintains a channel at an authorized depth of 4.3 m underneath the recently-constructed Marc Basnight Bridge, which spans the inlet and opened to traffic in 2019. The south side of the inlet was previously stabilized in 1991 through the construction of a terminal groin that extends under the southern terminus of the bridge. A well-developed flood delta extends approximately 5 km into the sound and includes a network of shoals and channels, and a corresponding ebb delta extends approximately 3.5 km offshore (Figure 1).

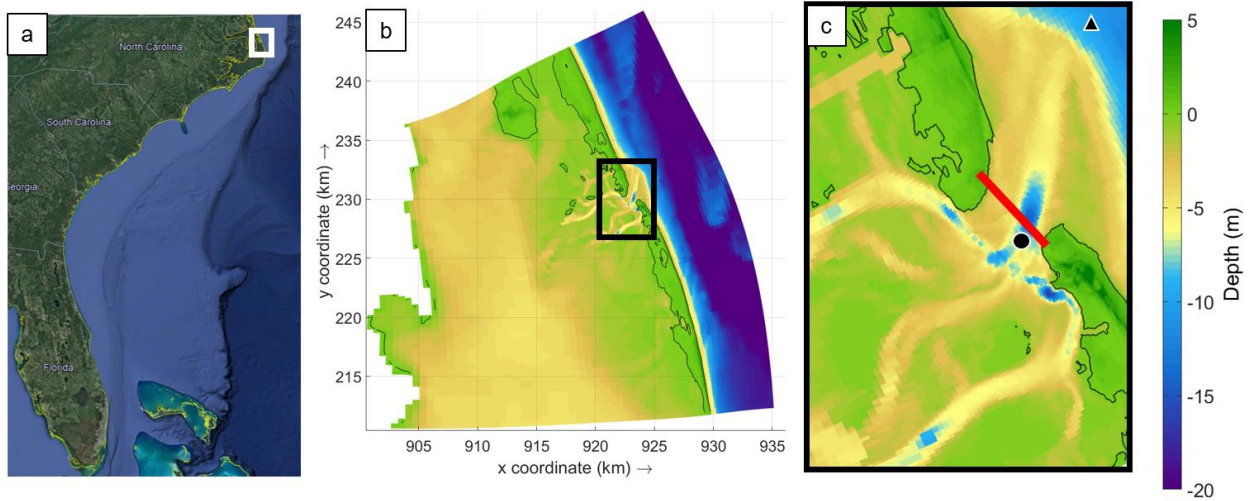


Figure 1. (a) Location of Oregon Inlet relative to the southeast coast of the United States; (b) and (c) model domain. The red transect and black dots on panel (c) are synthetic monitoring locations in the simulations.

Oregon Inlet, like the entire Outer Banks barrier island system, is subject to frequent storm events that impact navigation ability in the main inlet channel and shape the formation of both the flood and ebb tidal deltas and channels. Hurricanes and tropical storms occur in the summer and fall months while frequent nor'easter storms dominate the winter months, contributing to a seasonal wave climate that drives the overall dynamics of the inlet and surrounding barrier islands.

Storms can approach Oregon Inlet from the ocean, sound, and mainland. Here, we focus on sound-side or, more broadly, bay-side storms. One of these storms, Hurricane Irene, made landfall in North Carolina on August 27, 2011, as a Category 1 storm. Following a track through Albemarle-Pamlico Sound, the storm generated maximum water levels up to 2.1 m (NAVD 88). Documented impacts of Irene included sound side flooding and barrier island breaching (Clinch et al., 2012; Overton and Smyre, 2013).

### 3. Methods

The numerical model Delft3D (Lesser et al., 2004) coupled with the wave model SWAN (Booij et al., 1999) are used to calculate hydrodynamic and wave conditions for Oregon inlet

during a tide-only scenario and a bay-side synthetic storm with conditions similar to those generated by Hurricane Irene (2011). The model has two subdomains with increased resolution near the inlet where cell sizes are 15 m (Figure 1). The bathymetry of the model was interpolated from a U.S. Army Corps of Engineers (USACE) hydrographic survey completed in the fall of 2019. Bathymetric and topographic datasets from the National Oceanographic and Atmospheric Administration (NOAA) were used in areas further from the inlet.

The hydrodynamic model has 5 open boundaries; the ocean boundary is forced with predicted and observed water levels at the NOAA station Duck (ID: 8651370), and the two lateral boundaries on the bay side are forced with water levels from the NOAA station Oregon Inlet Marina (ID: 8652587) in the north boundary and U.S. Coast Guard (USCG) station Hatteras (ID: 8654467) in the south boundary. The lateral boundaries in the ocean side are defined as Neumann boundaries with zero water level gradient. Waves are neglected for the tide-only scenario and set to a maximum of 7 m during the peak of the storm scenario. Other details of the model set up can be found in Velasquez-Montoya et al. (2020). The timeseries of boundary conditions are shown in Figure 2.

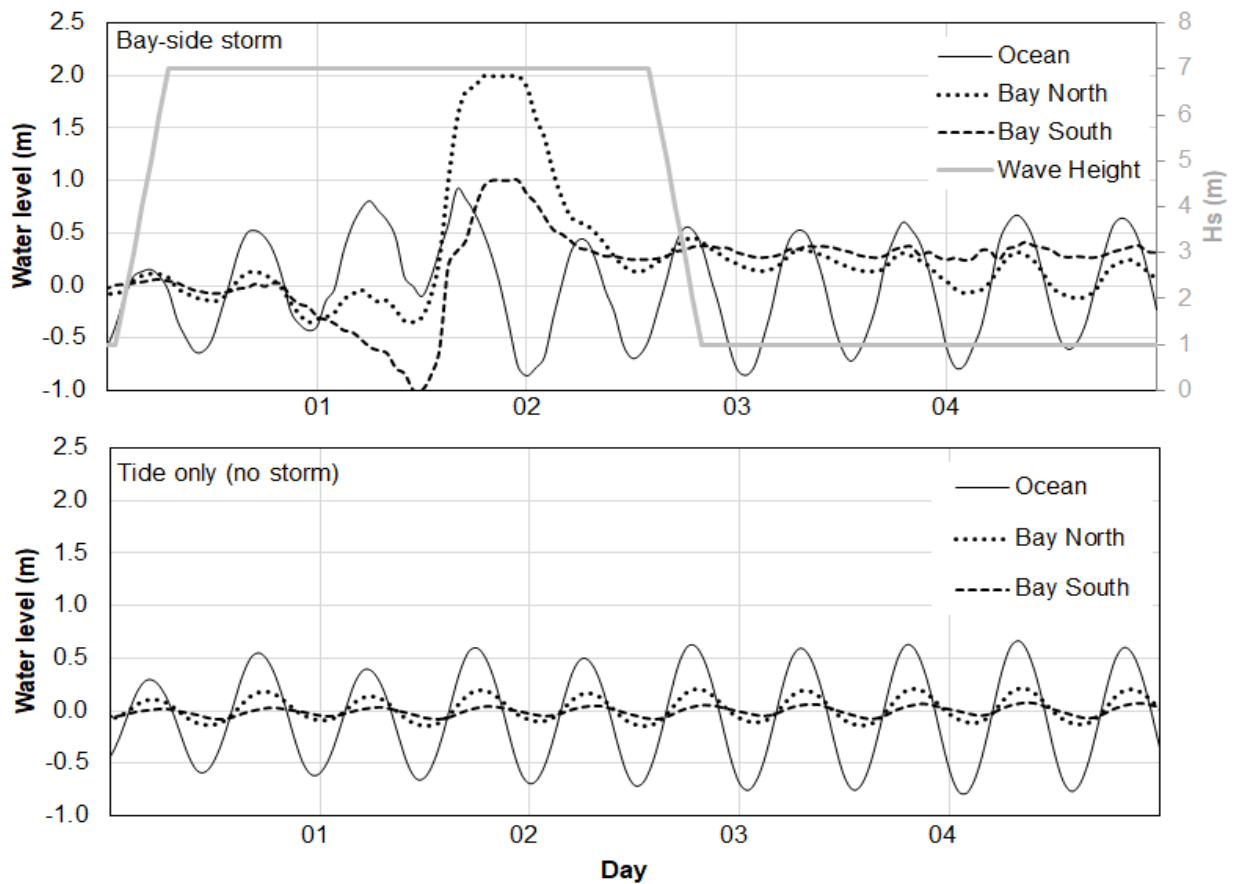


Figure 2. Boundary conditions for the bay-side storm and tide-only simulations

Time series of model outputs from the two scenarios (tide-only and bay-side storm) are analyzed at locations in the center of the inlet (black circle, Figure 1) and towards the ebb delta in the ocean side (black triangle, Figure 1). Inlet discharge is computed across the center of the inlet in the red transect shown in Figure 1. The variability of flooding extent and depth-averaged velocities are analyzed by means of spatiotemporal maps before, during, and after the peak of the storm. Difference maps of depth averaged velocities are used to indicate areas of enhanced or reduced flow velocities in the inlet due to the bay-side storm.

#### 4. Results

Prior to the arrival of the surge from the bay-side storm ( $t < 1.7$  days), the 7 m ocean-side waves (blue dash-dotted curve, Figure 3(b)) enhance flooding into the inlet (black curve, Figure 3(c)) and increase inlet water levels (black curve, Figure 3(a)) relative to the tide-only scenario. This wave impact increased each tidal cycle until the arrival of the bay-side storm surge, which changed the discharge from flood- to ebb-directed over a period of 3 hours and extended the duration of ebb-directed discharge from the semidiurnal duration of 6.4 hr to 9.7 hr.

Although the impact of the bay-side surge on instantaneous volumetric rate is significant, integrating over the entire course of the storm from the time the ocean-side waves arrive ( $t = 0$ ) to when the bay-side storm passes by the inlet and the waves die down ( $t = 2.8$  days) results in a negative (flood-directed) residual of  $-3.8 \times 10^8 \text{ m}^3$ , suggesting that, overall, waves dominated in driving water into the inlet. Once the waves die down, it takes another 49 hours for discharge through the inlet to balance out (i.e., residual volume = 0 from the  $t = 0$  to 49 hours after the waves die down at  $t = 4.8$  days). Once the waves die down, the excess volume forced into the inlet during the storm is let out slowly through the extension of the ebb duration as well as an increase in the ebb discharge magnitude relative to the tide-only scenario.

Figure 4 shows the flooding extent and depth-averaged velocities for the bay-side storm (column 1) vs. tide only or no storm conditions (column 2) at three different moments of the tidal cycle (rows). The flooding extent during rising tide is constricted to tidal creeks connected to the bay, while the maximum flooding occurs during high and falling tide in the back side of the barrier islands. For this type of storm, the model did not indicate major flooding on the ocean side of the barrier islands; instead, all flooding occurs along the back-barrier region.

As expected, for rising and falling tides, the depth-averaged velocities during storm conditions are enhanced relative to the tides only scenario. During the rising tide, storm-driven currents in the inlet's main channel and meandering channels in the flood delta can be 2 m/s faster than under the tide-only simulation. At high tide when the flow begins to turn towards ebb, waves temporarily slow down ebbing currents in the inlet (blue shades in row 2, column 3 in Figure 4). During falling tide, the 2 m/s increase in currents occurs towards the main channel and ebb delta.

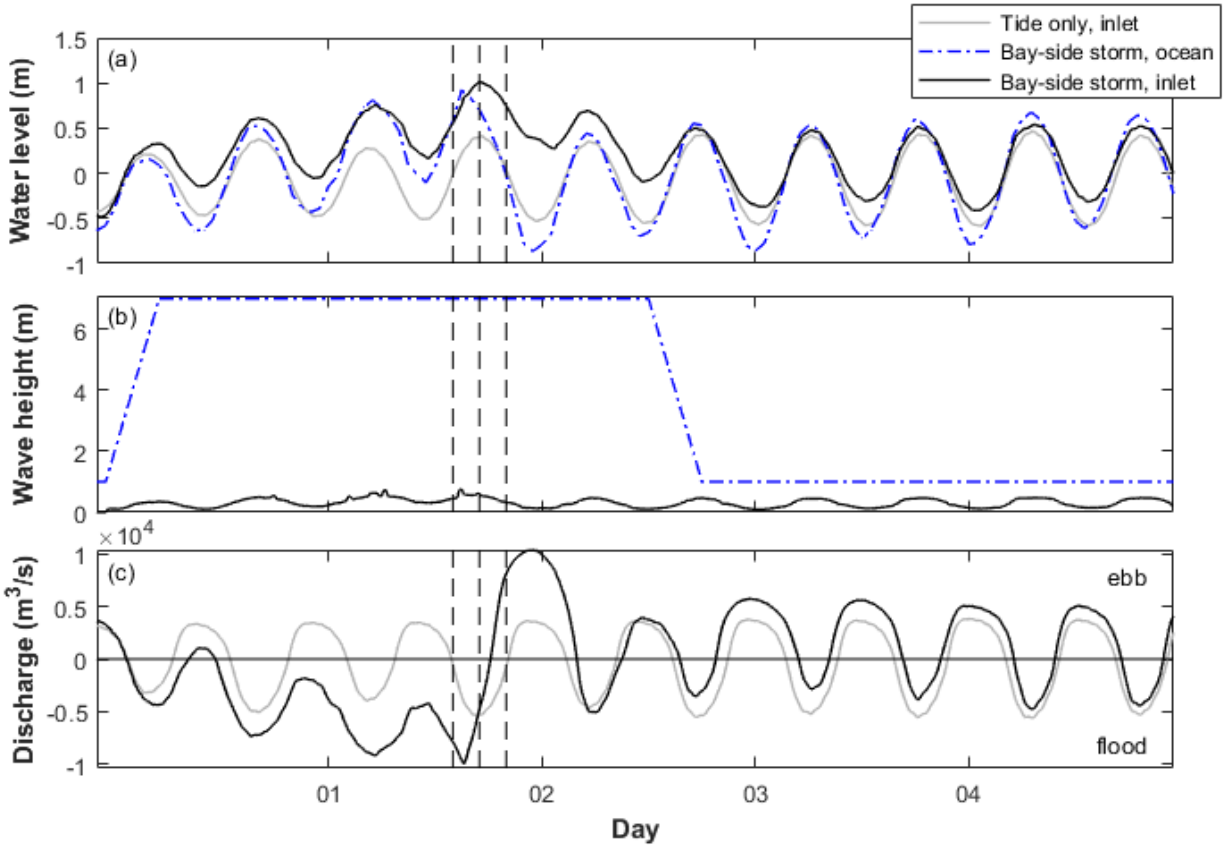


Figure 3. (a) Water level, (b) wave height, and (c) discharge through Oregon Inlet versus time. Black and gray curves show results during the bay-side storm scenario and the tides-only scenario, respectively, inside the inlet (water levels and wave heights at the black circle, Figure 1; discharge across the red transect in Figure 1). Blue dash-dotted curves show results off the ebb shoal (black triangle, Figure 1) during the bay-side storm scenario. Vertical dashed black lines indicate the times shown in Figure 4, from left to right, the rising tide, high tide, and falling tide, respectively.

These results indicate that during bay-side storms, waves and water level gradients between the bay and the ocean enhance flood currents for ~1.5 days in the initial phase of the storm. During this initial phase, water levels at the inlet are higher than under the tide-only simulation, however, there is no significant flooding around the barrier islands. As the storm moves north and water levels become higher in the bay compared to the ocean, outflow from the bay dominates ebb discharge, lasting more than 2 days. The maximum flooding extent occurs during peak ebb, only affecting the back-barrier region.

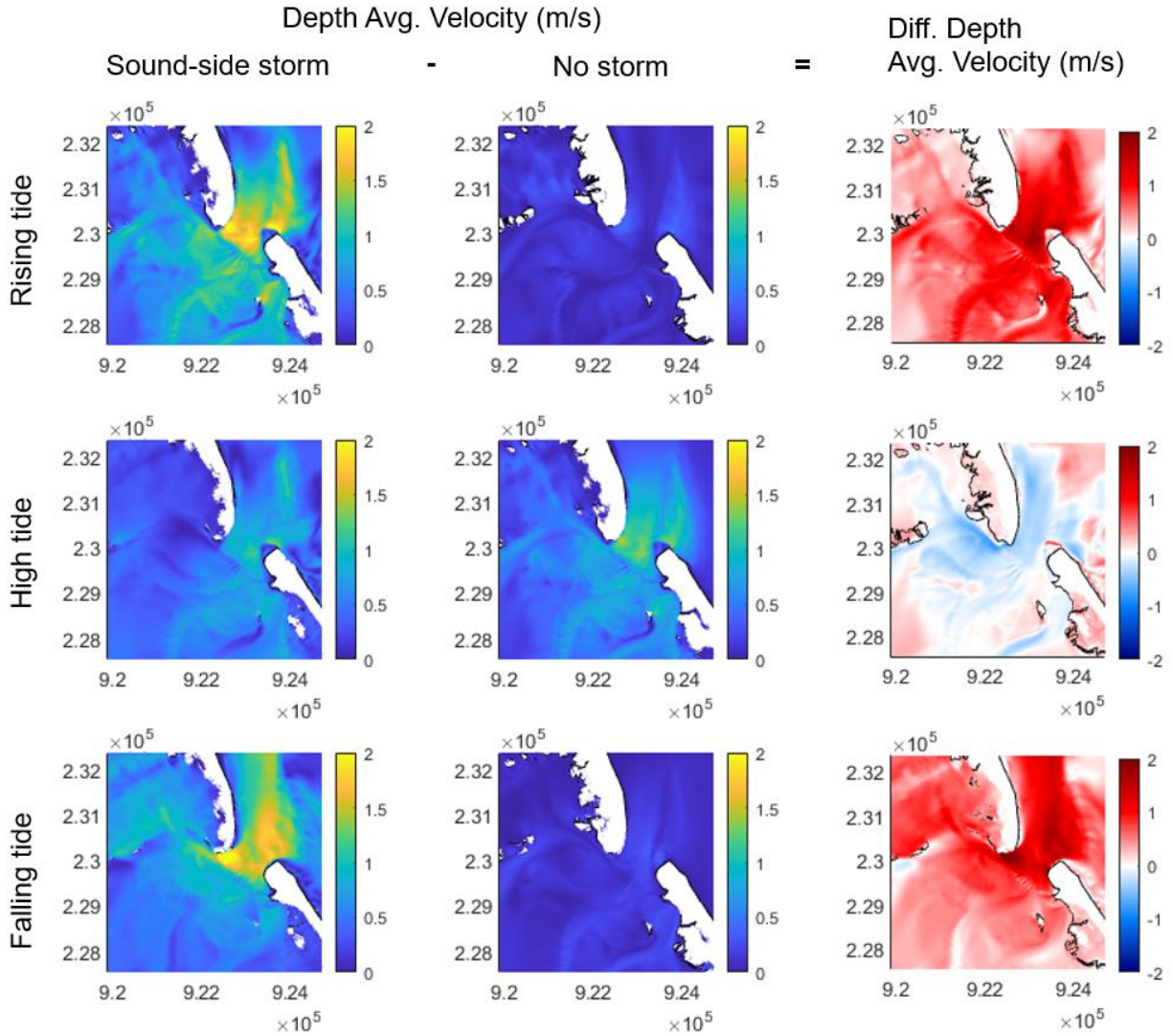


Figure 4. Spatial distribution of depth-averaged velocities before (top), during (middle) and after (bottom) peak of the water levels under a sound-side storm (column 1) and no storm conditions (column 2). Column 3: Spatial distribution of differences in depth averaged velocity between the sound-side storm and no storm conditions. Red colors indicate higher velocities during storm conditions than during only tides, blue colors indicate the opposite.

## 5. Discussion

The comparison of the hydrodynamic response of Oregon Inlet to a tide-only scenario and a bay-side storm allowed for estimation of changes in duration, extreme water levels, and currents at the inlet. It is expected that a coastal inlet will have different responses to extreme conditions that disturb the ocean or the bay. The results from this study indicate that during a bay-side storm, a tidal inlet can still funnel wave setup into the bay during the initial phase of the storm and during peak flood, but the enhanced water levels in the bay relative to the ocean drive fast ebb currents ( $> 2$  m/s) that rapidly overcome wave effects within the inlet.

The results presented here also indicate widespread flooding in the back-barrier region, which does not necessarily occur during ocean-side storms. The waves and surges from ocean-side storms are known to cause flooding and morphological changes mostly within oceanfront beaches and dunes. On the other hand, bay-side storms could lead to different consequences in the back-barrier region, which is typically composed of low-lying marshlands. Such consequences include marsh edge erosion and barrier island breaching driven by paleo-inlet channels present in large bays.

This study indicates that often overlooked bay-side storms could pose land and infrastructure management challenges different from those caused by ocean-side storms, thus highlighting the need for better understanding of the role and response of tidal inlets to this type of storm. Understanding the hydrodynamic and morphological processes associated with these events is especially important, because tidal inlets could act as the main coastal feature releasing excess water from rivers and bays. Future work will include analysis of different bay-side storms with varying water levels and waves. The results from this study will inform bay-side vulnerabilities of a coastal highway, as well as back barrier regions in front of large bays during extreme events.

### **Acknowledgements and Disclaimer**

This project was funded by the North Carolina Department of Transportation (NCDOT). The contents of this paper reflect the views of the author(s) and not necessarily the views of the Universities and Dewberry. The authors are responsible for the facts and the accuracy of the data presented herein. The contents do not necessarily reflect the official views or policies of either the North Carolina Department of Transportation or the Federal Highway Administration at the time of publication. This report does not constitute a standard, specification, or regulation.

### **References**

- Bruun, P., 1978. *Stability of Tidal Inlets: Theory and Engineering*. Elsevier.
- Booij, N., Ris, R.C., Holthuijsen, L.H., 1999. A third-generation wave model for coastal regions: 1. Model description and validation. *Journal of Geophysical Research* 104, 7649–7666, <http://dx.doi.org/10.1029/98JC02622>.
- Clinch, A., Russ, E., Oliver, R., Mitasova, H., Overton, M., 2012. Hurricane Irene and the Pea Island Breach: Pre-storm site characterization and storm surge estimation using geospatial technologies. *Shore & Beach* 80(2), 38–46.
- Dodet, G., Bertin, X., Bruneau, N., Fortunato, A., Nahon, A., Roland, A., 2013. Wave-current interactions in a wave-dominated tidal inlet. *Journal of Geophysical Research* 118, 1587–1605. <https://doi.org/10.1002/jgrc.20146>
- Elko, N., McKenna, K., Briggs, T. R., Brown, N., Walther, M., York, D., 2020. Best management practices for coastal inlets. *Shore & Beach*, 88(3), 75–83. <http://doi.org/10.34237/1008838>

- Hopkins, J., Elgar, S., Raubenheimer, B., 2018. Storm Impact on Morphological Evolution of a Sandy Inlet. *Journal of Geophysical Research: Oceans*, 213(8), 5751–5762. <https://doi.org/10.1029/2017JC013708>
- Irish J. L. and Cañizares, R., 2009. Storm-wave flow through tidal inlets and its influence on bay flooding. *Journal of Waterway, Port, Coastal and Ocean Engineering*, 135(2), 52–60. [https://doi.org/10.1061/\(ASCE\)0733-950X\(2009\)135:2\(52\)](https://doi.org/10.1061/(ASCE)0733-950X(2009)135:2(52))
- Keulegan, G. H., 1967. “Tidal Flow in Entrances Water-Level Fluctuations of Basins in Communications with Seas,” Technical Bulletin No. 14, Committee on Tidal Hydraulics, U.S. Army Engineer Waterways Experiment Station, Vicksburg, MS.
- Lesser, G.R., Roelvink, J.A., van Kester, J.A.T.M., Stelling, G.S., 2004. Development and validation of a three-dimensional morphological model. *Coastal Engineering*, 51, 883–915, <http://dx.doi.org/10.1016/j.coastaleng.2004.07.014>.
- Olabarrieta, M., Warner, J. C., Kumar, N., 2011. Wave-current interaction in Willapa Bay. *Journal of Geophysical Research: Oceans*, 116(12), 1–27. <https://doi.org/10.1029/2011JC007387>
- Orescanin, M., Raubenheimer, B., Elgar, S., 2014. Observations of wave effects on inlet circulation. *Continental Shelf Research*, 34(1), 37–42. <https://doi.org/10.1016/j.csr.2014.04.010>
- Overton, M., Smyre, E., 2013. Coastal Observations: Evolution of the Pea Island Breach, Outer Banks, North Carolina, *Shore & Beach*, 81(4), 23–27.
- de Swart, H.E., Zimmerman, J.T.F., 2009. Morphodynamics of Tidal Inlet Systems. *Annual Review of Fluid Mechanics*, 41, 203–29. <https://doi.org/10.1146/annurev.fluid.010908.165159>
- Wargula, A., Raubenheimer B., Elgar, S., Chen, J., Shi, F., Traykovski, P., 2018. Tidal Flow Asymmetry Owing to Inertia and Waves on an Unstratified, Shallow Ebb Shoal. *Journal of Geophysical Research: Oceans*, 213(9), 6779–6799. <https://doi.org/10.1029/2017JC013625>
- Velasquez-Montoya, L., Overton, M. F., Sciaudone, E. J., 2020. Natural and anthropogenic-induced changes in a tidal inlet: Morphological evolution of Oregon Inlet. *Geomorphology*, 350(2020), 106871 1-8. <https://doi.org/10.1016/j.geomorph.2019.106871>